Experimental verification of a micromagnetic model of dual-layer magnetic films

John O. Oti and Stephen E. Russek
Electromagnetic Technology Division, National Institute of Standards and Technology, Boulder, Colorado 80303

A micromagnetic model has been used to characterize the magnetic properties of dual-layer magnetic films. The model calculations, with experimentally determined input parameters, have been compared with measurements on fabricated Co alloy dual-layer films. Calculations are done with a more general version of a previous micromagnetic model, modified to allow the variation of certain media parameters which were previously held constant. Each of the experimental media consists of a bilayer of 30-nm-thick $Co_{0.75}Ni_{0.25}$ magnetic films separated by a Cr decoupling layer. The calculations predict a split in the coercivities of the layers for small Cr thicknesses which is observed experimentally. The model correlates an observed increase in media squareness ratio and coercivity, as the Cr thickness is increased, with diminishing exchange and magnetostatic interactions between the magnetic layers.

I. INTRODUCTION

Interest in multilayer cobalt-alloy longitudinal recording films stems from the reduced media noise and increased output they exhibit compared to single-layer films, a property which makes them attractive for high-density recording applications.[1] A micromagnetic model for simulating dual-layer films was recently described.[2] The model is capable of simulating layers with different magnetic and geometric properties, and includes interlayer exchange interaction effects between the layers. Although useful information about the magnetization processes in the films is obtained using this model, it still represents an oversimplification of the complex microstructural and micromagnetic properties of a real film. Actual film grains come in a range of shapes, sizes, and orientations, and are coupled magnetically with each other in a complex manner that varies across the medium.[3]

In this work we outline a generalization of the model described in Ref. 2, which incorporates a distribution of certain coupling parameters that were previously treated as constants. The generalized model is then used to replicate major hysteresis loop characteristics of fabricated dual-layer Co-Ni films, using experimentally obtained model parameters. The model calculations give variations of coercive field, coercive field splitting, and squareness with magnetic film separation that are in qualitative agreement with experimental data. The model calculations further give insight into the mechanisms leading to the observed variations in film magnetic properties.

II. MICROMAGNETIC MODEL

The micromagnetic model simulates two magnetic layers, one on top of the other, designated as top and bottom layers, respectively. The layers are discretized into two-dimensional uniform arrays of single-domain parallelopiped elements, representing the grains of the medium. The layers are separated by a nonmagnetic decoupling layer. Each layer is characterized by a magnetic anisotropy distribution, and the elements interact with each other by magnetostatic, and nearest-neighbor exchange interactions. The magnetic layers are coupled by magnetostatic and exchange interactions. The response of the medium to an applied field is obtained by simultaneously integrating a system of coupled Landau–Lifschitz equations[2,4] written for all the elements of the medium.

We introduce a new formulation of the effective magnetostatic and exchange interaction fields. Unlike the approach of Ref. 2, this formulation contains coupling constants that are variable quantities. The equations that follow are written for the top layer alone, and the subscripts t and b are used to denote quantities in the top and bottom magnetic layers. The corresponding expressions for the bottom layer are obtained from these by interchanging the roles of t and b in the equations. The reduced magnetostatic and exchange interaction fields acting on an element in the top are given by

$$\mathbf{h}_{mt}=\sum_{j=1}^{N} C_{ht}(x_j,y_j)\sum_{k=1}^{6}\hat{\mathbf{n}}_{jkt}\cdot\hat{\mathbf{m}}_{jt}\mathbf{G}_{jkt}+\sum_{j=1}^{N} C'_{ht}(x_j,y_j)\sum_{k=1}^{6}\hat{\mathbf{n}}_{jkb}\cdot\hat{\mathbf{m}}_{jb}\mathbf{G}'_{jkb} \quad (1)$$

and

$$\mathbf{h}_{et}=\sum_{j=1}^{\mathrm{nn}} C_{et}(x_j,y_j)\hat{\mathbf{m}}_{jt}+C'_{et}(x_j,y_j)\hat{\mathbf{m}}_b\,. \quad (2)$$

Equations (1) and (2) are expressed as the sums of two terms; the first represents the interactions among elements of the top layer, and the second represents interactions in the top layer due to elements of the bottom layer. Primed quantities are used to distinguish interlayer coupling constants from those for interactions among elements of the same layer. The sources of the magnetostatic interaction field are the magnetic surface charges induced on the bounding faces of the elements due to their uniform magnetization. The inner summation in Eq. (1) accounts for the six bounding faces of an element; the upper limit nn of the summation in Eq. (2) indicates that the summation is over the four nearest neighbors of the element in the top

layer; N is the total number of elements in each magnetic layer; $\hat{\mathbf{n}}_{jkt}$ is the unit outward normal of the kth face of the jth neighbor; $\mathbf{G}_{jk}$ and $\mathbf{G}'_{jk}$ are vector Green's functions which depend on the mutual orientation of the elements;[2] $C_{ht}=M_t/(4\pi H_{kt})$ and $C'_{ht}=M_b/(4\pi H_{kt})$ are the magnetostatic coupling constants which vary with position as a result of variations in the anisotropy field distribution $H_{kt}(x_j,y_j)$, of the top layer; M_t, and M_b are the magnetization of the top and bottom layers and are constant for all elements of the same layer; C_{et} and C'_{et} are phenomenological exchange coupling constants and are functions of position.

The method followed in this article for simulating real media is to first estimate average values of the coupling constants ($\langle C_{ht}\rangle$, $\langle C_{et}\rangle$, etc.) and then assign to the elements parameters chosen at random from an interval about these averages. The average values are found by the formulas in Ref. 2, that is, using constant parameters. The average magnetostatic coupling constant is obtained from experimental data, but the average exchange coupling constant is chosen as one that yields a sufficiently close match between experimental and calculated loops.

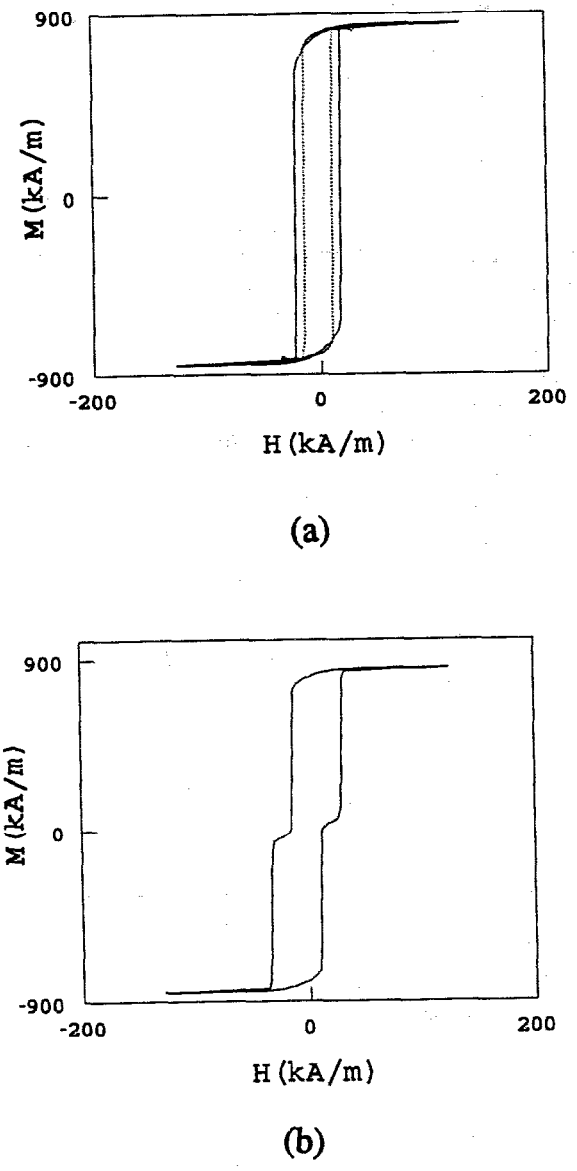

FIG. 1. Calculated loops of the $d=20$ nm dual-layer medium: (a) top layer (solid curve) and bottom layer (dashed curve); (b) composite loop.

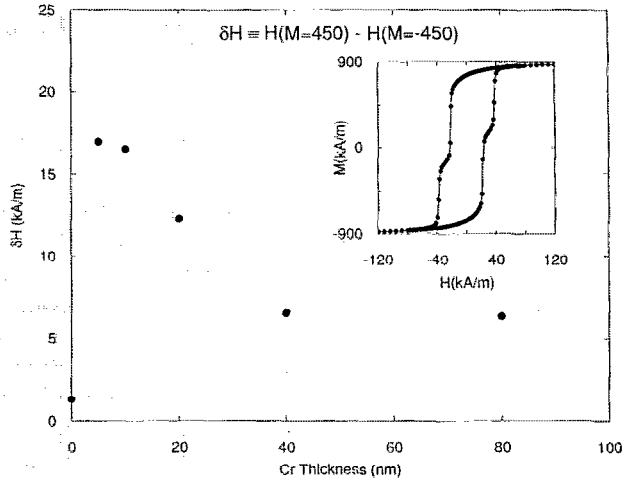

FIG. 2. Experimental coercive field splitting δH as function of Cr thickness d.

III. EXPERIMENT

Experimental multilayer thin-film structures were fabricated by sputtering. Commercial (100) silicon wafers with 300 nm thermal SiO_2 grown on top were used as substrates. First a 50 nm Cr adhesion layer was rf sputter deposited on the substrate. Then a magnetic dual layer was fabricated by dc magnetron cosputtering a 30 nm $Co_{0.75}Ni_{0.25}$film, rf sputtering a Cr decoupling layer, and cosputtering a top 30 nm $Co_{0.75}Ni_{0.25}$ film. The thickness of the Cr decoupling layer was varied as $d=0$, 5, 10, 20, 40, and 80 nm. All depositions were done on room-temperature substrates. The base pressure of the sputtering chamber was typically 2.6×10^{-6} Pa (2×10^{-8} Torr). Experimental M-H loops were measured with a superconducting quantum interference device (SQUID) magneto-

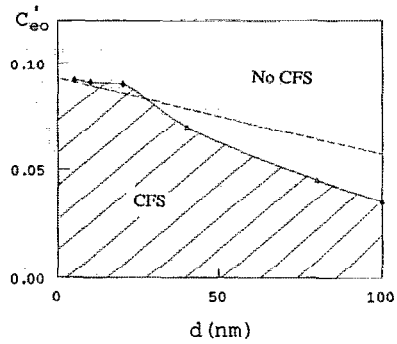

FIG. 3. Interlayer exchange constant C'_{e0} as function of Cr thickness d. ♦ and Δ denotes the limiting exchange constants obtained for $d<40$ nm and $d\geq40$ nm, respectively. The dashed line is an estimate of the true exchange constant variation.

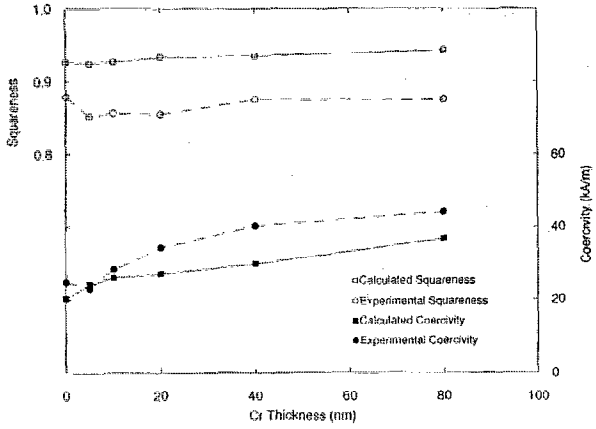

FIG. 4. Calculated (solid curves) and experimental (dashed curves) squareness ratio S and coercivity H_c as functions of Cr thickness d.

meter. The parameters used in the calculations are chosen by first matching the major loop of the single-layer medium ($d=0$). To simulate the single layer, two magnetic layers with similar magnetic properties as the single-layer medium, but far enough from each other as to act independently, are used. Interlayer exchange interactions are neglected for this calculation. The parameters obtained for the single layer were then used in simulating the dual-layer media.

An element size of 22 nm is used in the calculations. This is the median grain size from a histogram of grain sizes obtained from a scanning tunneling microscope image of the surface of a dual-layer film sample. The sample has a saturation magnetization of $M_s=860$ kA/m and an anisotropy field of $H_k=193$ kA/m (2420 Oe), similar to other cobalt-nickel films.[5] These values yield estimates of the average magnetostatic coupling constants of $C_{h0}=\langle C_{ht,b}\rangle=\langle C'_{ht,b}\rangle=M_s/(4\pi H_k)=0.36$.

We performed x-ray-diffraction studies with standard radial and asymmetric radial scans on the (10.0), (10.1), and (10.3) peaks; these indicated the absence of strong texture in the films. To a first approximation this implies an isotropic distribution of film grains and hence of their c axes and magnetic anisotropy axes.

IV. SIMULATION RESULTS AND DISCUSSION

In the calculations each magnetic layer is modeled as a 20×20 array of tightly packed elements, with the anisotropy axes randomly oriented in both layers. Periodic boundary conditions are used. For some of the results presented below we repeated the calculations using larger array sizes up to a 50×50 array without noticing any appreciable change in the results. Landau–Lifschitz equations with infinite damping (neglecting precession) are used to describe the gyromagnetic behavior of the elements. The magnetostatic coupling constants are assigned at random among the elements from the interval 0.95 C_{h0} to 1.05 C_{h0}. A close fit of the experimental loop was achieved with the exchange coupling constant values randomly distributed among the elements from the interval 0.95 C_{e0} to 1.05 C_{e0} where $C_{e0}=\langle C_{et,b}\rangle=0.47$. The M-H loops are measured with H in the plane of the films. The squareness ratio of the calculated loop is 5% more than the experimental value of 0.88, and the calculated coercivity is 20% less than the experimental value of 24.5 kA/m (308 Oe).

Calculated loops for the $d=20$ nm film are shown in Fig. 1, where a hump appears in the composite curve due to differences in coercivities of the layers. The experimental loops also display similar coercive field splitting (CFS) for $d<40$. The experimental CFS width δH is plotted as a function of d in Fig. 2. This behavior was seen in all our calculations for the considered range of d when the interlayer exchange interactions between the layers were neglected. This suggests that the magnetostatic interactions are primarily responsible for the formation of the CFSs. The magnetization of the layers reverses by the formation and mobility of vortices.[2] The vortices minimize the magnetostatic energy of the layer by providing magnetization flux closure. The vortices begin to form at different times in both layers because the distributions of their magnetic properties, although similar, are not identical. Once formed in a given layer, the vortices frustrate the formation of vortices in the second layer. This causes the magnetization reversals of the layers to occur at different times.

As shown in Ref. 2, a large enough exchange interaction between the layers would cause them to reverse their magnetization in unison, resulting in the equality of their coercivities but not necessarily of their squareness ratios. For each film, calculations in which the average interlayer exchange coupling constant $C'_{e0}=\langle C'_{et}\rangle=\langle C'_{eb}\rangle$ was gradually increased from zero up to a value at which the CFS just disappeared were carried out. Figure 5 shows plots of exchange constants as functions of Cr thickness. The data points represent the values obtained as described above. They lie at the boundary of the region of CFS and no CFS. We assume that for $d<40$ nm, C'_{e0} is overestimated since in this region the CFSs do exist in the experimental curves, and for $d\geqslant40$ nm they are underestimated since they correspond to the onset of the disappearance of the CFSs. Consequently the true variation of C'_{e0} should lie below the data points when d is approximately less than 40 nm and above the data points when d is greater than approximately 40 nm, and should decrease monotonically. We approximate this line by the dashed line of Fig. 3, which is the average of the tangents drawn from both ends of the boundary curve. The coercivities and squareness ratios calculated using constants obtained from the dashed line are compared with experimental data in Fig. 4.

[1] S. E. Lambert, J. K. Howard, and I. L. Sanders, IEEE Trans. Magn. **MAG-25**, 2706 (1990).
[2] J. Oti, IEEE Trans. Magn. (in press).
[3] T. Chen, IEEE Trans. Magn. **MAG-17**, 1181 (1981).
[4] J. C. Mallinson, IEEE Trans. Magn. **MAG-23**, 2003 (1987).
[5] M. R. Khan, S. Y. Lee, J. L. Pressesky, D. Williams, S. L. Duan, R. D. Fisher, N. Heiman, M. R. Sheinfein, J. Unguris, D. T. Pierce, R. J. Celotta, and D. Seliotis, IEEE Trans. Magn. **MAG-26**, 2715 (1990).